

Promotion and Mitigation of Premixed Flame Acceleration in Dusty-Gaseous Environment with Various Combustible Dust Distributions: A Computational Study

Sinan Demir, Hayri Sezer, Torli Bush, and V'yacheslav Akkerman*

Center for Alternative Fuels, Engines and Emissions (CAFE)

Center for Innovation in Gas Research and Utilization (CIGRU)

Computational Fluid Dynamics and Applied Multi-Physics Center (CFD&)

Department of Mechanical and Aerospace Engineering, West Virginia University

Morgantown, WV 26506-6106

1 Introduction

Accidental explosions of flammable gases due to combustible dust impurities may result in injuries and deaths, as well as the destruction of expensive equipment, thereby constituting an important demand in the industries dealing with explosive materials such as the coalmining industry, which historically has one of the highest fatality and injury rates. While combustion of gaseous fuels has been studied reasonably well, as well as that of combustible dust particles, the process of flame propagation in a combined dusty-gaseous environment, especially with a non-uniform dust distribution in a gas, remains almost as an enigma that commands both the fundamental interests and practical relevance.

A planar premixed flame front propagates with a speed S_L , but such a flame rarely occurs in reality. Indeed, the majority of industrial and laboratory flames are usually corrugated due to turbulence, acoustics, shocks, combustion instabilities, wall friction, in-built obstacles etc. A curved flame front has a larger surface area relative to a planar one; therefore, it consumes more fuel per unit time and releases more heat, thereby propagating faster than the planar flame front. Consequently, a flame should accelerate with a continuous increase in the flame surface area. One of the well-known mechanisms of flame acceleration is that by Shelkin [1], associated flame acceleration due to nonslip boundary conditions at the walls. Namely, as a flame front propagates from a closed tube/channel end, the burning matter expands; it pushes a flow of the fresh fuel mixture; friction at the pipe walls makes the flow non-uniform, which bends the flame front, increasing its velocity and associated acceleration. The idea was subsequently developed, theoretically and numerically, by Bychkov et al [2] for spatially-constant thermal-chemical flame-fuel properties (such as S_L). However, in reality, S_L may experience spatial and temporal variations, caused by non-uniform distributions of an equivalence ratio or dust impurity within a coalmine.

With this work we initiate a systematic study on how local variations of the thermal-chemical flame and fuel properties may influence the global flame evolution. In this particular study, we consider dusty-gaseous environment and focus on flame acceleration due to wall friction. Specifically, the computational simulations of the compressible hydrodynamic and combustion equations are performed, with the combustible coal dust particles incorporated into the original CFD platform by means of the classical Seshadri formulation [3]. Namely, a real dusty-gaseous environment is replaced by an “effective” gaseous fluid with locally-modified, dust-induced flow and flame parameters. Keeping in mind a coalmine passage as a potential application, we consider flame propagation in a pipe with large aspect ratio. For simplicity, the two-dimensional (2D) planar Cartesian geometry is employed. Various coal dust concentration distributions are studied, namely: (a) homogenous, (b) linear, (c) cubic and (d) parabolic. While homogenous distribution simply gives a scaling factor as compared to the gaseous case [2], non-uniform distributions are anticipated to provide qualitatively new features. As a result, we identified the similarity

and differences in evolution of the flame shape morphology and flame propagation velocity in each case. It is shown that a non-uniform dust distribution may result in extra distortion or local stabilization of the flame front, which promotes or reduces the total flame front surface area, thereby facilitating or moderating flame acceleration induced by wall friction.

2 Computational Platform

The core of the computational platform consisted of a fully-compressible, finite-volume Navier-Stokes code solving for the hydrodynamics and combustion equations in gaseous environment. It was adapted to parallel computations and validated on numerous reactive flow and aero-acoustic problems [4-5]. The basic equations read:

$$\frac{\partial}{\partial t} \rho + \frac{\partial}{\partial x_i} (\rho u_i) = 0, \quad \frac{\partial}{\partial t} (\rho u_i) + \frac{\partial}{\partial x_j} (\rho u_i u_j + \delta_{i,j} P) - \gamma_{i,j} = 0, \quad (1)$$

$$\frac{\partial}{\partial t} \left(\rho \varepsilon + \frac{1}{2} \rho u_i u_j \right) + \frac{\partial}{\partial x_i} \left(\rho u_i h + \frac{1}{2} \rho u_i u_j u_j + q_i - u_j \gamma_{i,j} \right) = 0, \quad (2)$$

$$\frac{\partial}{\partial t} (\rho Y) + \frac{\partial}{\partial x_i} \left(\rho u_i Y - \frac{\zeta}{Sc} \frac{\partial Y}{\partial x_i} \right) = -\frac{\rho Y}{\tau_R} \exp(-E_a/R_p T), \quad (3)$$

where Y is the mass fraction of the fuel mixture, $\varepsilon = QY + C_v T$ the internal energy, $h = QY + C_p T$ the enthalpy, Q the energy release in the reaction, C_v, C_p the heat capacities at constant volume and pressure, respectively. We consider a single irreversible reaction of the first-order and that of the Arrhenius type, with the activation energy E_a and the constant of time dimension τ_R . The stress tensor $\gamma_{i,j}$ and the energy diffusion vector q_i are given by

$$\gamma_{i,j} = \zeta \left(\frac{\partial u_i}{\partial x} + \frac{\partial u_j}{\partial x_i} - \frac{2}{3} \frac{\partial u_k}{\partial x_k} \delta_{i,j} \right), \quad q_i = -\zeta \left(\frac{C_p}{Pr} \frac{\partial T}{\partial x_i} + \frac{Q}{Sc} \frac{\partial Y}{\partial x_i} \right), \quad (4)$$

where $\zeta \equiv \rho \nu$ is the dynamic viscosity, Pr and Sc the Prandtl and Schmidt numbers, respectively. Later, we implemented combustible dust particles into this solver by using the Seshadri formulation [3] that expresses the laminar burning velocity, $S_{d,L}$, as a function of local thermal-chemical properties of the gas and coal dust in the form

$$S_{d,L} = \frac{1}{Ze} \sqrt{\frac{2Bk_u}{\rho_u C_T} \exp\left(-\frac{E_a}{R_u T_f}\right)}, \quad Ze = \frac{E_a (T_f - T_u)}{R_u T_f^2}, \quad (5)$$

where E_a is the activation energy, Ze the Zel'dovich number, and

$$C_T = C_p + C_s n_s \frac{4\pi r_s^3}{3} \frac{\rho_s}{\rho}, \quad (6)$$

the entire specific heat capacity of the mixture, with C_s being that of the coal dust particles, respectively. Here ρ is the density of the mixture, which can be expressed as $\rho = \rho_u + c_s$, where ρ_u is the fresh gas density and c_s the concentration of particles. The quantity $n_s = (c_s / \rho_s) / V_s$ is the number of particles per unit volume, with $V_s = 4\pi r_s^3 / 3$ being the volume of a single particle and r_s the radius of this particle. The flame speed is promoted by the effect of volatiles released from the coal particles through the gaseous mixture, which is accounted as an additional fuel source for the combustion process in the reaction zone.

As a result, the growth of the equivalence ratio promotes the flame temperature (T_f^*) and, thereby, the flame propagation speed ($S_{d,L}^*$); see [3,6] for details.

We utilize the computational platform developed to investigate the impact of various combustible dust distributions on the scenario of flame acceleration induced by wall friction. In fact, coal dust distribution is typically non-uniform in coalmines [7]. Indeed, a stationary dense coal dust layer may spread through the bottom of the channel. Initially, a gaseous-based detonation wave may produce a strong shock that can lift and entrain the dust layer. Over time, the shock weakens but the shock-heated air is ignited by lifted dust [7]. Hence, a second combustion process is initiated in the presence of gas-air and non-uniform dust mixture. In this manner, a lifted dust layer may resemble a linear, cubic, or even parabolic distribution due to different energy levels of complex magnetic forces. This may justify our choice of dust distributions, specified below, though it is difficult to identify a realistic distribution of coal particles in a coalmine.

The four distributions considered are presented in Fig. 1. First, we employed a uniform coal dust distribution (Fig. 1a), which provides a base model for the computational platform. Subsequently, we consider three non-uniform dust distributions along the channel as functions of a radial coordinate. In the case of linear dust distribution, Fig. 1b, we have the maximum coal dust concentration, $c_{s,max}$, at the bottom of the channel and no dust at the top of the channel. By applying the boundary conditions on the linear gradient of non-uniform dust distribution, we end up with the function

$$c_s = c_{s,max} (1 - x / 2R). \quad (7)$$

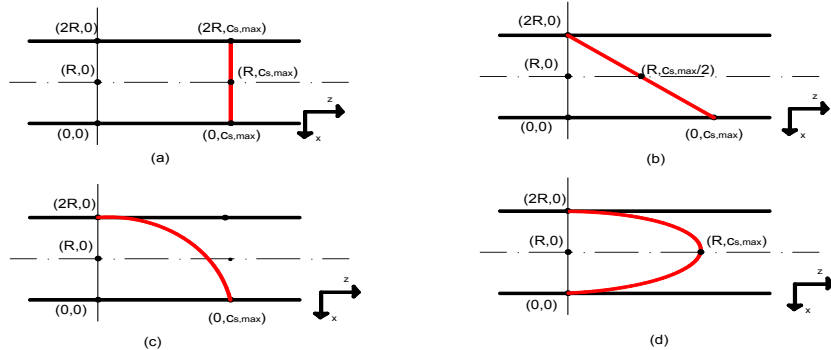


Figure 1. Schematic illustration of the different dust concentration distribution gradients. Homogenous (a); linear (b); cubic (c) and parabolic (d) coal dust concentration distribution.

We also considered a cubic coal dust distribution,

$$c_s = c_{s,max} \left[1 - (x / 2R)^3 \right], \quad (8)$$

as illustrated in Fig. 2c. Finally, we employed a parabolic dust distribution,

$$c_s = c_{s,max} \left[1 - 4((x - R) / 2R)^2 \right], \quad (9)$$

depicted in Fig. 1d, where the dust concentration is at maximum along the centerline, and is zero (no dust) along the bottom and top of the channel. With $x = 0$, all Eqs. (7) – (9) obviously yield $c_s = c_{s,max}$ (Fig. 1a).

In the present simulations, we considered lean ($\phi = 0.7$) methane-air-coal dust combustion, which is relevant to practical reality. Additionally, a small particle radius ($r_s = 10\mu\text{m}$), which provides an effective equivalence ratio promotion due to fast pyrolysis ability, is used, with a concentration of 120g/m^3 . The laminar flame speed for the given equivalence ratio ($\phi = 0.7$) in the absence of dust particles was taken as

$S_L = 0.169\text{m/s}$ [8]. This value provides realistically slow flame propagation as compared to the speed of sound (the flame Mach number, $Ma = S_L / c_0$, is 4.87×10^4). In fact, this flame velocity can be calculated by

using Eq. (5) with $c_s = 0$ or $r_s = 0$. The thermal expansion in the burning process is determined by the energy release in the reaction and defined as the density ratios of fuel to burnt matter, $\Theta = \rho_u / \rho_b$; we took $\Theta = 6.11$, which is related to methane-coal particle burning for the given equivalence ratio, ($\phi = 0.7$) [8]. We took the standard (“room”) initial pressure and temperature, $P_f = 10^5 \text{ Pa}$ and $T = 300 \text{ K}$. The dynamic viscosity (ζ) and the Prantdl number Pr were taken as $1.7 \times 10^{-5} \text{ Ns/m}^2$ and 1.0, respectively, with the Lewis number being $Le = \text{Pr} / Sc = 1.0753$. The gas mixture is a perfect gas of a constant molecular weight $2.9 \times 10^{-2} \text{ kg/mol}$. In the gas phase, the equation of state is $P = \rho R_p T / m$. The activation energy was $E_a = 56 R_p T_f$. Flame dynamics are conventionally characterized by the Reynolds number associated with flame propagation

$$\text{Re} = \frac{RS_L^{mean}}{\nu} = \frac{R}{\text{Pr} L_f}, \quad (10)$$

where $L_f = 8.65 \times 10^{-5} \text{ m}$ is the thermal flame thickness and R the channel half-width. It was shown that the effect of non-uniform dust distribution becomes substantial when the channel width is no less than $\text{Re} = 24$, so we used this value of Re in the present simulations.

3 Result and Discussion

Figure 2 demonstrates the characteristic behavior of an accelerating flame for different dust distributions. Specifically, Fig. 2a shows the scaled flame tip velocity, U_{tip} / S_L versus the scaled time, $\tau = tS_L / R$. First of all, we observe linear flame acceleration for all distributions. The underlying reason for this trend is a relatively moderate thermal expansion ($\Theta = 6.11$) and relatively large Re , $\text{Re} = 24$, compared to Ref. [2], in which the flame acceleration mechanism competes with the combustion instabilities [9]. The test simulations showed that we gain an exponential acceleration regime for $\Theta = 8$ or more. Another interesting result is seen for the parabolic dust distribution, which moderates flame acceleration as compared to the homogeneous case. However, the most significant observations are the sudden jumps of the flame velocity, around $\tau = 0.24 \sim 0.26$, for linear and cubic distributions. Indeed, the flame velocity increases almost by an order of magnitude for methane-dust combustion, which might even lead to detonation for sufficiently fast flames, such as hydrogen-oxygen ones [2]. Also, the plots for linear and cubic distributions closely resemble each other. In Fig. 2b, the scaled flame front surface area, $A_w / 2R$, is given versus scaled time. As the flames surface area grows, so does its velocity. In the case of parabolic distribution, the lower flame surface area mitigates flame acceleration as depicted in Fig. 2a.

But what mechanism is responsible for such a trend? In order to answer this question, we investigate the evolution of the flame shape for all distributions at identical time intervals as shown in Fig. 3. For all simulation runs, the flame is imitated in the form of an initially planar front propagating in a semi-open channel from the closed end to the open one. Subsequently, the flame front gets corrugated due to wall friction and thereby non-uniform flow velocity field. In the homogeneous distribution, we observe the formation of a trough, which gets stronger over time, but afterwards the center part of the flame accelerates faster than upper and lower parts (please see also Fig. 2a.). At the end, only a small through is visible. After this point, we are unable to continue the simulations. The origin of the trough may be attributed to the hydrodynamic flame instability (the Darrieus-Landau; DL) allowable by the considered Re number [2]. Non-uniform distribution of the coal particles makes the flame shape much more intriguing. Specifically, the linear and cubic concentration distributions of particles lead to the formation of an asymmetric flame front, due to a higher concentration of combustible coal particles in the lower half

of the channel. Acceleration is strong in the lower branch in all directions so that it catches the upper part later on. The snapshots of the flame evaluation show that the trough formation and loss of symmetry of the flame front is originated in the region close to the flame cusp.

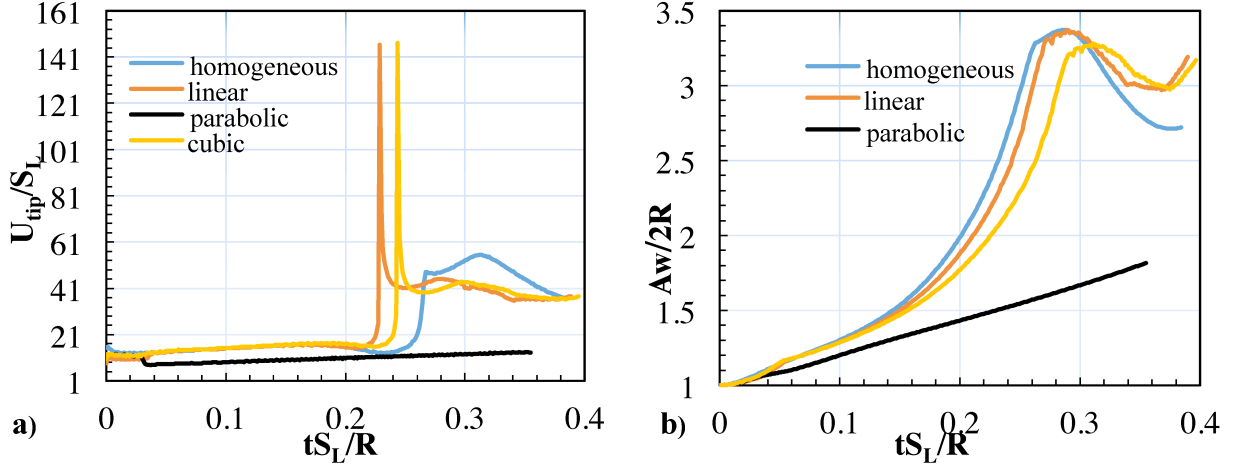


Figure 2. Scaled propagation speed of the flame tip (a); scaled flame surface area (b) versus the scaled time S_{Lt}/R for various coal dust distribution gradients.

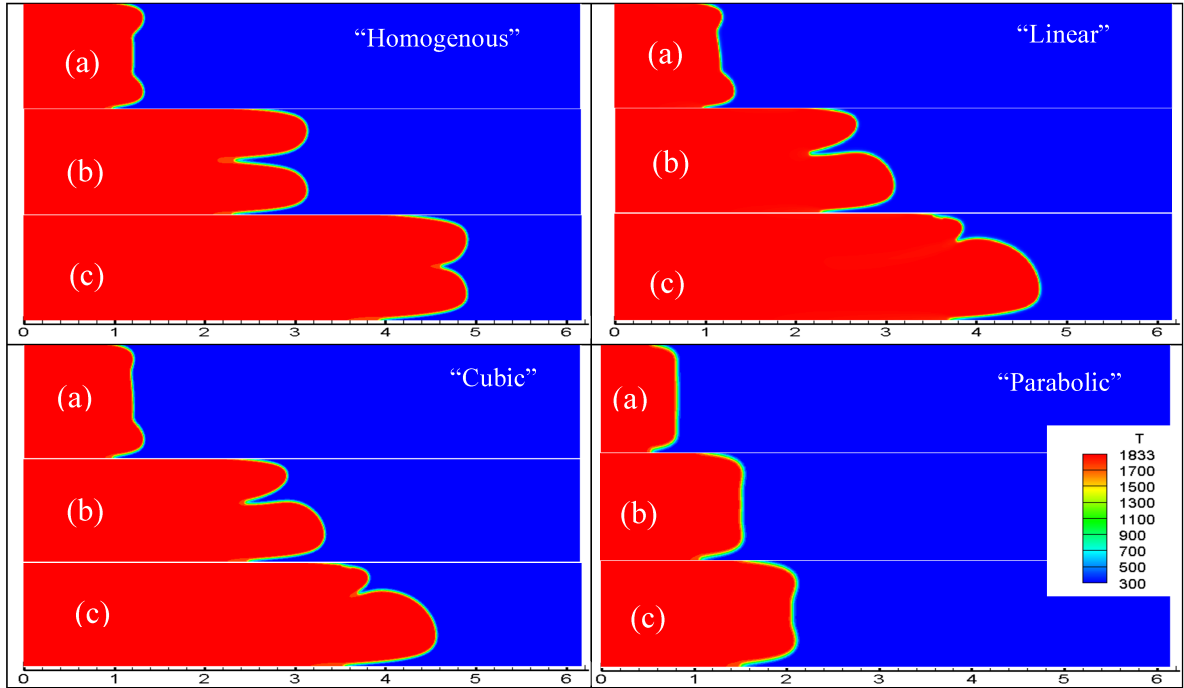


Figure 3. Temperature field evolution in a channel of half-width $R = 24L_f$: $\tau = 0.15$ (a), $\tau = 0.27$ (b), $\tau = 0.36$ (c).

Finally, let us discuss the effect of parabolic dust concentration distribution. As one may remember, in this case, the dense combustible particles are distributed through the center of the channel while their concentration decreases towards the upper and lower sidewalls. After ignition of the fuel mixture, an intrinsically unstable flame front tries to generate a trough as observed for the homogeneous distribution. However, centrally located dust particles promote the flame velocity, locally, and thereby prevent a trough formation. In other words, the parabolic distribution of the combustible particles stabilizes an

intrinsically unstable flame front. Consequently, the increase in the flame surface area appears slower thereby moderating flame acceleration as compared to other distributions considered. One important point to be noted is the cases of non-symmetric flame fronts, as observed in linear and cubic distributions. In fact, the flames do not have a "tip" at the centerline in that case such that Fig. 2a simply plots the time evolution of the flame coordinate at the centerline. This point will be elucidated in future studies.

4 Summary

In the present paper, we have investigated flame propagation in a combined dusty-gaseous environment with non-uniform coal dust distributions by means of computational simulations. It is shown that a non-uniform dust distribution may result in extra distortion or local stabilization of the flame front, which increases or decreases the total flame front surface area, thereby promoting or moderating the flame acceleration scenario. In a future study, we aim to investigate later stages of flame acceleration due to wall friction that may provide other significant remarks. Moreover, the effect of the particle radius, concentration and different distribution functions can also be examined in a set of parametric simulations. It would also be interesting to investigate the effect of inert particles and their distributions. A reader may expect to see validation of the provided computational platform. Unfortunately, we are not aware of any experimental studies and hope that the present study will provide a good platform for more elaborated experiments for combustion of non-uniformly distribution of coal particles. Consequently, we believe that this study yields considerable physical insights not only for accidental coalmine flames but also for applications to utilize combustion by developing controlling strategies.

References

- [1] Shelkin K. (1940). Influence of tube walls on detonation ignition. *Zh. Eksp. Teor. Fiz.* 10: 828.
- [2] Bychkov V, Petchenko A, Akkerman V, Eriksson LE. (2005). Theory and modelling of accelerating flames in tubes. *Phys. Rev. E.* 72: 046307.
- [3] Seshadri K, Berlad AL, Tangirala V. (1992). The structure of premixed particle-cloud flames. *Combust. Flame.* 89:342.
- [4] Valiev D, Bychkov V, Akkerman V, Law CK, Eriksson LE. (2010). Flame acceleration in channels with obstacles in the deflagration-to-detonation transition. *Combust. Flame.* 157: 1021.
- [5] Petchenko A, Bychkov V, Akkerman V, Eriksson LE. (2007). Flame–sound interaction in tubes with nonslip walls. *Combust. Flame.* 149: 434.
- [6] Xie Y, Raghavan V, Rangwala AS. (2012). Study of interaction of entrained coal dust particles in lean methane-air premixed flames. *Combust. Flame.* 159: 2456.
- [7] Houim RW, Oran ES. (2015). Numerical simulation of dilute and dense layered coal-dust explosions. *Proc. Combust. Inst.* 35: 2090.
- [8] Davis SG, Quinard J, Searby G. (2002). Markstein Numbers in Counterflow, Methane- and Propane-Air Flames: A Computational Study. *Combust. Flame.* 130: 136.
- [9] Demirgok B, Ugarte O, Valiev D, Akkerman V. (2015). Effect of thermal expansion on flame propagation in channels with nonslip walls. *Proc. Combust. Inst.* 35: 936.